

Modulation and enhancement of photonic spin Hall effect with graphene in broadband regions

Peng Dong(董鹏), Gaojun Wang(王高俊), and Jie Cheng(程杰)

Citation: Chin. Phys. B, 2021, 30 (**3**): 034202. DOI: 10.1088/1674-1056/abccb2
Journal homepage: http://cpb.iphy.ac.cn; http://iopscience.iop.org/cpb

What follows is a list of articles you may be interested in

Plasmonic characteristics of suspended graphene-coated wedge porous silicon nanowires with Ag partition

Xu Wang(王旭), Jue Wang(王珏), Tao Ma(马涛), Heng Liu(刘恒), and Fang Wang(王芳)
Chin. Phys. B, 2021, 30 (**1**): 014207. DOI: 10.1088/1674-1056/abb65c

Tunable dual-band terahertz graphene absorber with guided mode resonances

Jun Wu(吴俊), Xia-Yin Liu(刘夏吟), and Zhe Huang(黄喆)
Chin. Phys. B, 2021, 30 (**1**): 014202. DOI: 10.1088/1674-1056/abaee2

An ultrafast and low-power slow light tuning mechanism for compact aperture-coupled disk resonators

Bo-Yun Wang(王波云), Yue-Hong Zhu(朱月红), Jing Zhang(张静), Qing-Dong Zeng(曾庆栋), Jun Du(杜君), Tao Wang(王涛), Hua-Qing Yu(余华清)
Chin. Phys. B, 2020, 29 (**8**): 084211. DOI: 10.1088/1674-1056/ab9df1

Low-power electro-optic phase modulator based on multilayer graphene/silicon nitride waveguide

Lanting Ji(姬兰婷), Wei Chen(陈威), Yang Gao(高阳), Yan Xu(许言), Chi Wu(吴锜), Xibin Wang(王希斌), Yunji Yi(衣云骥), Baohua Li(李宝华), Xiaoqiang Sun(孙小强), Daming Zhang(张大明)
Chin. Phys. B, 2020, 29 (**8**): 084207. DOI: 10.1088/1674-1056/ab943b

Orbit-orbit interaction and photonic orbital Hall effect in reflection of a light beam

Zhang Jin, Zhou Xin-Xing, Ling Xiao-Hui, Chen Shi-Zhen, Luo Hai-Lu, Wen Shuang-Chun
Chin. Phys. B, 2014, 23 (**6**): 064215. DOI: 10.1088/1674-1056/23/6/064215

Modulation and enhancement of photonic spin Hall effect with graphene in broadband regions*

Peng Dong(董鹏)[1,2,3], Gaojun Wang(王高俊)[1], and Jie Cheng(程杰)[2,†]

[1] College of Electronic and Optical Engineering & College of Microelectronics, Nanjing University of Posts and Telecommunications, Nanjing 210023, China
[2] School of Science, New Energy Technology Engineering Laboratory of Jiangsu Province, Nanjing University of Posts and Telecommunications, Nanjing 210023, China
[3] Key Laboratory of Radio Frequency and Micro-Nano Electronics of Jiangsu Province, Nanjing 210023, China

(Received 8 October 2020; revised manuscript received 7 November 2020; accepted manuscript online 23 November 2020)

The photonic spin Hall effect (SHE) holds great potential applications in manipulating spin-polarized photons. However, the SHE is generally very weak, and previous studies of amplifying photonic SHE were limited to the incident light in a specific wavelength range. In this paper, we propose a four-layered nanostructure of prism-graphene-air-substrate, and the enhanced photonic SHE of reflected light in broadband range of 0 THz–500 THz is investigated theoretically. The spin shift can be dynamically modulated by adjusting the thickness of air gap, Fermi energy of graphene, and also the incident angle. By optimizing the structural parameter of this structure, the giant spin shift (almost equal to its upper limit, half of the incident beam waist) in broadband range is achieved, covering the terahertz, infrared, and visible range. The difference is that in the terahertz region, the Brewster angle corresponding to the giant spin shift is larger than that of infrared range and visible range. These findings provide us with a convenient and effective way to tune the photonic SHE, and may offer an opportunity for developing new tunable photonic devices in broadband range.

Keywords: photonic spin Hall effect, graphene, spin shift

PACS: 42.25.–p, 41.20.Jb, 42.79.–e, 78.20.Ci **DOI:** 10.1088/1674-1056/abccb2

1. Introduction

The photonic spin Hall effect (SHE), first proposed by Onoda *et al.* in 2004,[1] is an interesting phenomenon, in which the left- and right-handed circularly polarized components can shift transversely perpendicular to the refractive index gradient,[1–4] when a light beam is reflected or transmitted from a planar dielectric interface. It can be regarded as a direct optical analogy of electronic SHE where the roles of the photon spin and refractive index gradient are similar to electron spin and electric potential, respectively.[1,4] The photonic SHE has been demonstrated to originate from an effective spin–orbit interaction,[3,5] governed by the conservation law of total angular momentum.[4,6,7] However, it is very hard to observe the photonic SHE directly, since the corresponding spin-dependent splitting is only on a subwavelength scale, usually about a few tens of nanometers. Until 2008, Hosten and Kwait first detected this tiny transverse displacement of refracted light at an air–glass interface by using a weak measurement technique to amplify the shift about 10^4 times.[8] Then the photonic SHE is attracting vast attention and has been widely investigated in many physical systems, including semiconductor physics,[9] optical physics,[10,11] metamaterials,[12] *etc*.[13–15]

Recently, effective methods to amplify the photonic SHE have become especially necessary, and the investigations on the large spin-dependent splitting were reported.[16–19] For example, the photonic SHE can be enhanced in layered nanostructure by just modulating the structure parameters.[11] Tang *et al.*[20] and Qiu *et al.*[21] revealed a giant in-plane photonic spin splitting of reflected light at the Brewster angle. A giant SHE of transmitted and reflected light was observed by using a thin epsilon-near-zero slab.[22,23] Meanwhile, surface plasmon resonance has also been proposed to enhance the photonic SHE shift.[24–26] Very recently, Zhou *et al.* revealed a flexible way to modulate and enhance the photonic SHE via exceptional points.[18] These interesting results suggest that the photonic SHE may offer new opportunities to manipulate photons and will open up possibilities for developing new photonic devices.

Graphene, a one-atom-thick planar sheet of carbon atoms arranged in a hexagonal honeycomb lattice,[27] has attracted enormous interest due to its unique electronic and optical properties. Its optical parameter can be dynamically tuned in a wide range by varying the Fermi energy through electrostatic doping.[28] In addition, graphene supports the surface plasmon in infrared and terahertz range with low loss compared with noble metals.[29] Therefore, graphene is very

*Project supported by the National Natural Science Foundation of China (Grant No. 11405089), the General Program of the Natural Science Foundation of Jiangsu Province, China (Grant No. BK20171440), the Postgraduate Research & Practice Innovation Program of Jiangsu Province, China (Grant No. SJKY19_0779), and the Natural Science Foundation of Nanjing University of Posts and Telecommunications, China (Grant Nos. NY218039 and NY220030).

†Corresponding author. E-mail: chengj@njupt.edu.cn

© 2021 Chinese Physical Society and IOP Publishing Ltd

promising material for developing new tunable photonic devices. In fact, the investigations of photonic SHE in graphene-based structure have been widely reported. Bai *et al.* theoretically modulated the spin shift of photonic SHE at a telecommunication wavelength by introducing a graphene layer. Results pointed out that the spin shift is quite sensitive near the Brewster angle and could be tuned by adjusting the Fermi energy of graphene.[30] Based on the relationship between the spin shift and the graphene layer number, Zhou *et al.* proposed the technique to identify the graphene layers by using the photonic SHE.[31] By varying Fermi energy of graphene and the thickness of the graphene metamaterial, the photonic SHE in a three-layer structure containing graphene metamaterial could be tunably enhanced when the wavelength of incident light was about 4.5 μm (infrared wavelength).[32] Moreover, the tunable and enhanced photonic SHE in a layered nanostructure containing two single sheets of graphene was explored at a terahertz wavelength.[33] Very recently, a simple and effective method was proposed to actively control the asymmetric photonic SHE by introducing the tunability of optical conductivity into graphene with an incident wavelength of 1550 nm.[34] However, the above explorations for amplifying photonic SHE were limited to the incident light of a specific wavelength range. To the best of our knowledge, the tunable and enhanced photonic SHE in broadband range are rarely reported.

In this work, we construct a four-layered nanostructure containing the prism, graphene, air gap and the substrate, in which the broadband photonic SHE is theoretically investigated. It is pointed out that the strong spin shift can be realized in a broadband range covering the terahertz, infrared and visible range. Moreover, the giant transverse splitting can reach up to its upper limitation (about half of beam waist) by adjusting the Fermi energy of graphene, the thickness of air gap and the incident angle.

2. Model and theory

A four-layered nanostructure (in Fig. 1) composed of the glass prism, monolayer graphene, an air gap and the substrate is proposed. In this structure, the refractive index of the glass prism and the silica substrate are both 1.5, and the thickness of air gap can be tuned and is denoted by d. For the condition of low temperatures, the monolayer graphene can be expressed by the optical conductivity σ as[35]

$$\sigma(\omega,E_{\rm f}) = \frac{e^2E_{\rm f}}{\pi\hbar^2}\frac{\rm i}{\omega+{\rm i}\tau^{-1}} + \frac{e^2}{4\hbar}\left[{\rm step}(\hbar\omega-2E_{\rm f}) + \frac{\rm i}{\pi}\ln\left|\frac{\hbar\omega-2E_{\rm f}}{\hbar\omega+2E_{\rm f}}\right|\right], \quad (1)$$

where ω is the angular frequency, step(x) is the Heaviside step function and it can be expressed as[36]

$$\text{step}(x) = \begin{cases} 1, & \text{if } x > 0, \\ 0, & \text{if } x < 0, \end{cases}$$

$\hbar$ is the Planck constant, $E_{\rm f}$ is the Fermi energy of graphene, $\tau = \mu E_{\rm f}/ev_{\rm f}^2$ is the relaxation rate relating to the mobility $\mu = 10^4\ {\rm cm^2\cdot V\cdot s^{-1}}$ and Fermi velocity $v_{\rm f} = 10^6\ {\rm m\cdot s^{-1}}$. The first and second terms in Eq. (1) stem from the intraband and interband contributions, respectively.

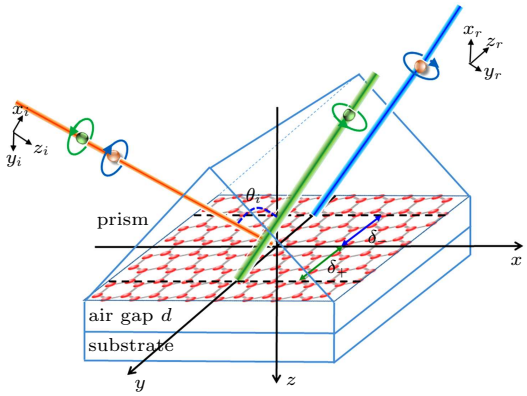


Fig. 1. Schematic diagram of photonic SHE of reflected light in four-layered structure of prism–graphene–air–substrate.

When a linearly polarized beam is incident from the glass prism to the surface of the multilayer structure at an angle θ_i, the reflected beam will split into left- and right-handed circularly polarized spin component whose centroids will shift reversely away from the incident plane. In our configuration, the incident plane is x–z plane and the transverse shift is along the y axis.

Here, we consider an incident Gaussian beam whose angular spectrum can be written as

$$\tilde{E}_i = \frac{w_0}{\sqrt{2\pi}}\exp\left[-\frac{(k_x^2+k_y^2)w_0^2}{4}\right], \quad (2)$$

where w_0 is the beam waist, k_x and k_y are the components of the wave vector along the x-axis and y-axis directions, respectively. The reflected angular spectrum is related to the boundary distribution of the electric field and can be expressed as follows:[11]

$$\begin{bmatrix}\tilde{E}_r^{\rm H}\\ \tilde{E}_r^{\rm V}\end{bmatrix} = \begin{bmatrix} r_{\rm p} & \dfrac{k_{ry}\cot\theta_i(r_{\rm p}+r_{\rm s})}{k_0} \\ -\dfrac{k_{ry}\cot\theta_i(r_{\rm p}+r_{\rm s})}{k_0} & r_{\rm s}\end{bmatrix} \times \begin{bmatrix}\tilde{E}_i^{\rm H}\\ \tilde{E}_i^{\rm V}\end{bmatrix}, \quad (3)$$

in which $\tilde{E}_r^{\rm H,V}$ and $\tilde{E}_i^{\rm H,V}$ are the H and V components of the angular spectrum with the reflected and incident beam, respectively, $r_{\rm p}$ and $r_{\rm s}$ are Fresnel reflection coefficient for p and s waves, k_0 is the wave number in free space, and k_{ry} is y component of reflected wave vector. Using the relationship $\tilde{\boldsymbol{E}}_i^{\rm H} = (\tilde{\boldsymbol{E}}_{i+} + \tilde{\boldsymbol{E}}_{i-})/\sqrt{2}$ and $\tilde{\boldsymbol{E}}_i^{\rm V} = i(\tilde{\boldsymbol{E}}_{i-} - \tilde{\boldsymbol{E}}_{i+})/\sqrt{2}$, we can obtain the reflected angular spectrum of left- (positive sign in

subscript) and right-handed (negative sign in subscript) circularly polarized component.

The transverse displacement of the reflected light beam is defined as

$$\delta^{\pm}_{\mathrm{H,V}} = \frac{\iint y \left| \boldsymbol{E}^{\pm}_{\mathrm{H,V}} \right|^2 \mathrm{d}x\mathrm{d}y}{\iint \left| \boldsymbol{E}^{\pm}_{\mathrm{H,V}} \right|^2 \mathrm{d}x\mathrm{d}y}, \tag{4}$$

where δ^{+} and δ^{-} represent the transverse displacement of left- and right-circularly polarized component, respectively. Considering the first-order Taylor series of the Fresnel coefficients, the spatial transverse spin-dependent shifts of the two spin components can be calculated as[24]

$$\delta^{\mathrm{H}}_{\pm} = \mp \frac{k_0 w_0^2 \mathrm{Re}(1+r_{\mathrm{s}}/r_{\mathrm{p}})\cot\theta_i}{k_0^2 w_0^2 + |\partial \ln r_{\mathrm{p}}/\partial\theta_i|^2 + |(1+r_{\mathrm{s}}/r_{\mathrm{p}})\cot\theta_i|^2}, \tag{5}$$

$$\delta^{\mathrm{V}}_{\pm} = \mp \frac{k_0 w_0^2 \mathrm{Re}\left(1+r_{\mathrm{p}}/r_{\mathrm{s}}\right)\cot\theta_i}{k_0^2 w_0^2 + |\partial \ln r_{\mathrm{s}}/\partial\theta_i|^2 + \left|\left(1+r_{\mathrm{p}}/r_{\mathrm{s}}\right)\cot\theta_i\right|^2}, \tag{6}$$

where $r_{\mathrm{p,s}} = |r_{\mathrm{p,s}}|\exp(\mathrm{i}\varphi_{\mathrm{p,s}})$, in which $\varphi_{\mathrm{p,s}}$ are the phases of Fresnel reflection coefficients $r_{\mathrm{p,s}}$. If $M = (1+r_{\mathrm{s}}/r_{\mathrm{p}})\cot\theta_i$, and considering that $\mathrm{Re}\,(M) \le |M|$, then the equations (5) can be simplified into

$$\begin{aligned}\delta^{\mathrm{H}}_{\pm} &= \mp w_0 \frac{k_0 w_0 \,\mathrm{Re}\,(M)}{k_0^2 w_0^2 + \left|\partial \ln r_{\mathrm{p}}/\partial\theta_i\right|^2 + |M|^2} \\ &\le \mp w_0 \frac{k_0 w_0 \,|M|}{k_0^2 w_0^2 + \left|\partial \ln r_{\mathrm{p}}/\partial\theta_i\right|^2 + |M|^2}.\end{aligned} \tag{7}$$

The maximum spin shift can be obtained when the following conditions are satisfied simultaneously: (i) the term of $|\partial \ln r_{\mathrm{p}}/\partial\theta_i|^2$ in the denominator is negligible and (ii) $k_0^2 w_0^2 = |M|^2$. Under these conditions, the maximum value of spin shift approaches closely to $w_0/2$ but cannot exceed it. And we can obtain the same result from Eqs. (6). Therefore, half of the incident beam waist is the upper limit of the spin shift.

As is well known, the spin shifts for left- and right-circularly polarized light are opposite in sign but the same in magnitude. Equations (5) and (6) are the main analytical formulas in this paper, and it is straightforward that the Fresnel coefficients are the crucial parameters to determine the spin shifts for the reflected beam. Transfer matrix method is a powerful tool in analyzing the light propagations and has been widely used to study optical properties.[37,38] Here, the Fresnel reflection coefficient for p and s waves can be determined by a 2×2 transfer matrix:[11]

$$M = T_{1\to 2} P_2 T_{2\to 3} P_3 \cdots P_m T_{m\to m+1}, \tag{8}$$

where

$$T_{m\to m+1} = \frac{1}{t_{m\to m+1}} \begin{bmatrix} 1 & r_{m\to m+1} \\ r_{m\to m+1} & 1 \end{bmatrix}$$

is the transmission matrix from the m-th layer to the $(m+1)$-th layer, and

$$P_m = \begin{bmatrix} \exp(\mathrm{i}k_{mz}d_m) & 0 \\ 0 & \exp(-\mathrm{i}k_{mz}d_m) \end{bmatrix}$$

is the propagation matrix for the m-th layer with thickness of d_m. The Fresnel reflection coefficients (r_{p} and r_{s}) are given by the elements of transfer matrix: $r_{\mathrm{p,s}} = M_{21}/M_{11}$.

For monolayer graphene, the Fermi energy can be easily tuned by bias voltage via electronic doping, which will change the graphene conductivity and thus varying the Fresnel reflection coefficient. Within the framework of transfer matrix method, the incident angle, the thickness of air gap, and the Fermi energy of graphene can effectively modulate the Fresnel coefficient of our proposed four-layered nanostructure, then the photonic SHE will be tuned simultaneously.

3. Results and discussion

In this section, we will investigate the strong spin shift in broadband range for H-polarized Gaussian beam with a beam waist of 30λ. The frequency range in our calculations is from 0 THz to 500 THz which covers the terahertz, infrared and visible range. Figure 2 shows the Fresnel reflection coefficients and spin shifts as a function of incident angle and the frequency of incident wave. Here, the Fermi energy of graphene is 0.3 eV and the thickness of air gap is chosen to be 400 nm. As shown in Figs. 2(a) and 2(b), both $|r_{\mathrm{p}}|$ and $|r_{\mathrm{s}}|$ change with the incident angle and incident frequency. Increasing the frequency of incident wave, the incident angle corresponding to $|r_{\mathrm{p}}| \to 0$ (*i.e.* the Brewster angle) decreases sharply, while it remains stable to about 33.5° when the incident frequency is higher than 30 THz. That is due to the dramatic change of the graphene conductivity and corresponding relative permittivity in the low frequency range (see in Fig. 3). From Eq. (4) it follows that the spin shift can be determined by the difference between the Fresnel reflection coefficient $|r_{\mathrm{s}}|$ and $|r_{\mathrm{p}}|$. A large reflection of s-polarized light and a small reflection of p-polarized light will result in a large spin shift of circularly-polarized light for H polarization input. Therefore, we observe the strong spin shift around the Brewster angle as shown in Fig. 2(c). It is worth noting that this strong spin shift is involved in a broadband frequency range which covers the terahertz, infrared and visible range. The only difference is that the Brewster angle of terahertz range ($\sim 50°$) becomes larger than that of infrared and visible range ($\sim 33.5°$). As a consequence, just by modulating the incident angle conveniently, the strong spin shift can be realized in broadband range of 0 THz–500 THz, which will facilitate the development of novel optoelectronic devices in broadband range. It should be noted that for the incident light of 400 THz–500 THz, there is another critical angle at which the value of $|r_{\mathrm{p}}|$ tends to be zero. However, the zero value of $|r_{\mathrm{s}}|$ occurs simultaneously around this critical angle, resulting in a very tiny value of spin shift.

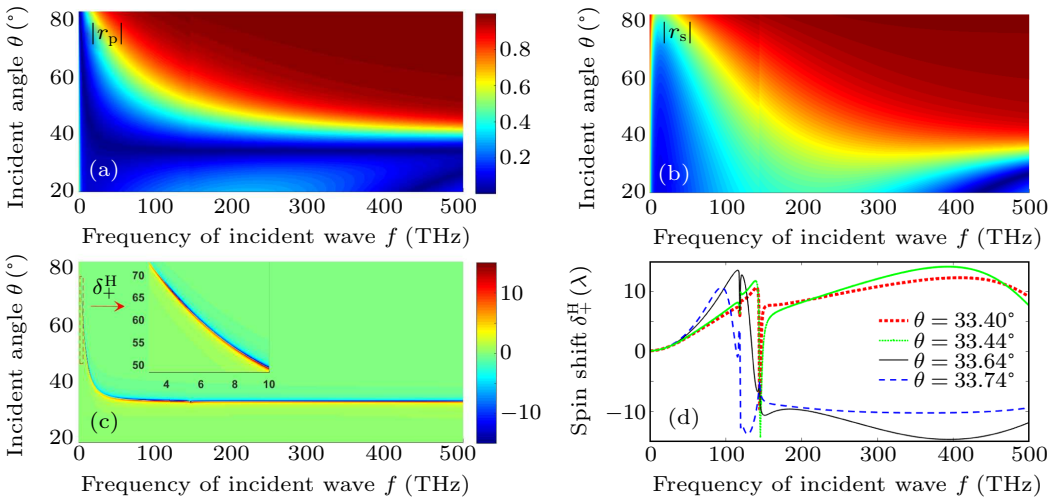


Fig. 2. Fresnel reflection coefficients (a) $|r_p|$, (b) $|r_s|$, and spin shift [(c) and (d)] changing with the incident angle θ and the frequency of incident wave. $E_f = 0.3$ eV, $w_0 = 30\lambda$, $d = 400$ nm.

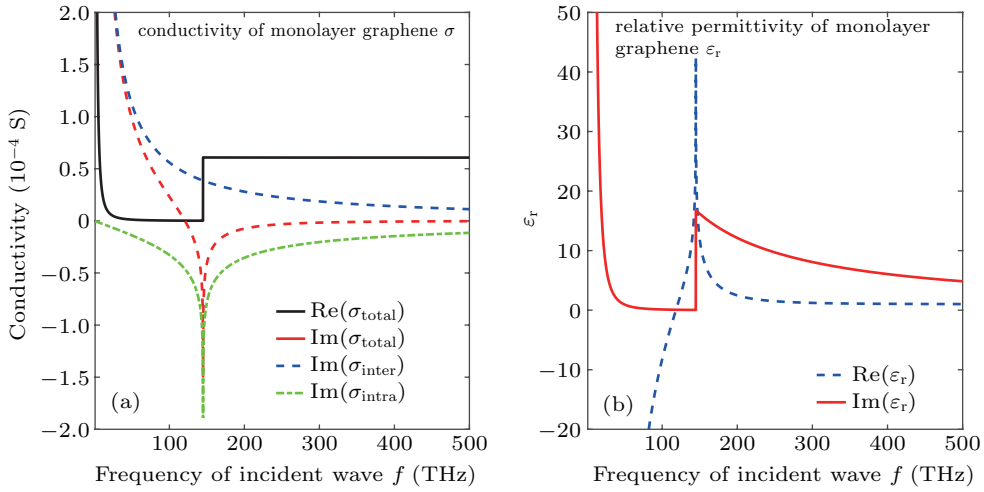


Fig. 3. Variations of (a) conductivity and (b) relative permittivity of monolayer graphene with incident wave frequency at Fermi energy of 0.3 eV.

To discuss the broadband spin shift in detail, the scenarios of four different incident angles are displayed in Fig. 2(d). For the incident angle of 33.40° and 33.44° , the positive spin shift is found to be about 8λ–13λ over a wide frequency range from 150 THz to 500 THz, while it turns into the negative value at 33.64° and 33.74° separately and the maximum spin shift can reach up to 15λ at 400 THz, which is almost equal to its upper limit. It should be noted that the photonic SHE is very interesting around these two special frequency points. One is at 120.8 THz, where the imaginary part of graphene conductivity is zero (as illustrated in Fig. 3), and a pronounced dip of the spin shift is induced. The other is around 144.8 THz, where real part of graphene conductivity shows a step-function-like increase and the imaginary part has a minimum, resulting in a sudden change of the spin shift at such an incident frequency.

The magnitude of spin shift is intimately related to the thickness of air gap in this layered structure, thus figure 4 shows the dependence of spin shift on thickness of air gap. Here, we choose three typical incident waves with wavelength $\lambda = 632.8$ nm (visible wavelength), 1550 nm (infrared wavelength), and 60 μm (terahertz range). It is interesting to note that the spin shift exhibits the periodic oscillations *versus* the thickness of air gap due to the Fabry–Perot resonance in the layered nanostructures.[11] From Figs. 4(b), 4(d), and 4(f), the optimal air thickness values for these three wavelengths are 0.52λ (or 1.42λ), 0.43λ (or 1.34λ) and 0.005λ (or 0.029λ), respectively. All the maximum spin shifts can reach to its upper limitation of 15λ. Furthermore, for the incident wavelength of 632.8 nm and 1550 nm, the giant spin shift is localized in a relatively narrow range of incident angle (about 33.5°), while in the terahertz range the Brewster angle for the strong spin shift varies greatly with the thickness of air gap. Generally speaking, with the decrease of the thickness of air gap, the Brewster angle increases monotonically. The minuscule air thickness will lead the Brewster angle to increase up to 80°. From the above analysis, the air gap of this layered nanostructure provides more flexibility for modulating the photonic SHE, and a giant spin shift can be achieved by optimizing the air thickness around the Brewster angle.

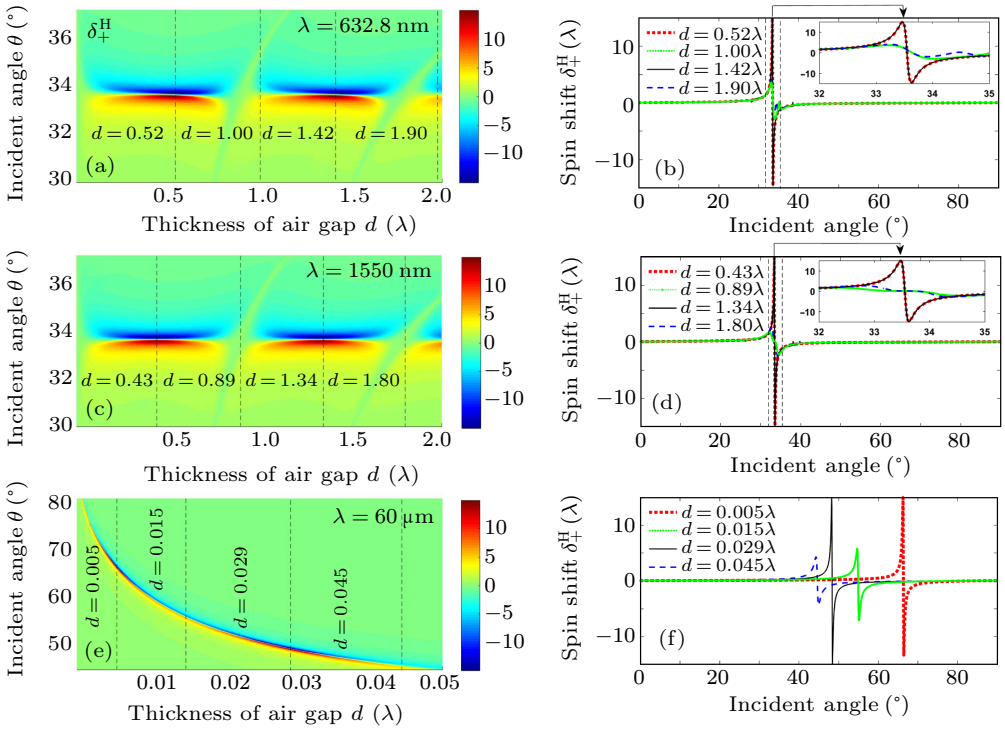


Fig. 4. Spin shifts changing with incident angle θ and the thickness of air gap d for three different incident wavelengths, with $E_f = 0.3$ eV and $w_0 = 30\lambda$.

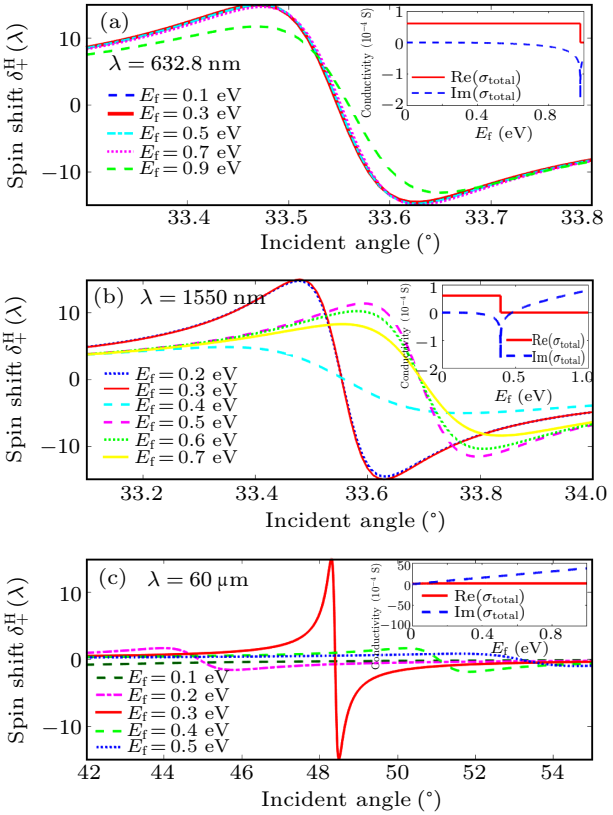


Fig. 5. Curves of spin shift *versus* incident angle with different values of Fermi energy of graphene for the incident wavelength of 632.8 nm, 1550 nm, and 60 μm, with insets displaying relation between conductivity of graphene and Fermi energy.

The Fermi energy of graphene can be modulated by bias voltage or electronic doping, which will tune the graphene conductivity σ (see Eq. (1)) and thus the Fresnel reflection coefficient. In order to reveal the influence of Fermi energy on the photonic SHE, the curves of spin shift *versus* the incident angle with different values of fixed Fermi energy of graphene are shown in Fig. 5. For the incident wavelength of 632.8 nm, as the Fermi energy of graphene is smaller than 0.7 eV, the spin shift is insensitive to E_f, due to the relatively stable conductivity of graphene. Continuing to increase the value of E_f to 0.9 eV, the value of spin shift becomes slightly decreased. For the case of 1550 nm, the spin shift is insensitive by adjusting the Fermi energy from 0.1 eV to 0.3 eV. With the Fermi energy increasing to 0.4 eV, the maximum value of spin shift drastically decreases to only 4λ, which is attributed to the step-function-like real part and the sudden dip of imaginary part of graphene conductivity. Then the spin shift increases to about 12λ as the Fermi energy is above 0.5 eV, accompanied by the larger Brewster angle of incident wave. Additionally, fixing the incident angle at 33.62° , the spin shift switches from negative to positive value with Fermi energy increasing. Moreover, the spin shift for the incident wave of 60 μm is very tiny with the E_f value of 0.2 eV, then it increases dramatically to the maximum value of 15λ under the condition of $E_f = 0.3$ eV. With the continuous increase of E_f, the value of spin shift then decreases sharply. It should be noted that for these three cases (*i.e.*, the incident wavelength of 632.8 nm, 1550 nm, and 60 μm), the different relations between the spin shift and E_f can be attributed to the variation in sensitivity of graphene conductivity to different wavelength of incident beam. But it is certain that the photonic SHE has a strong dependence on the graphene, and we can effectively control the spin shift by just adjusting the Fermi energy of graphene.

4. Conclusions

In this work, we theoretically investigate the tuning of the photonic SHE in a four-layered structure of prism–graphene–air–substrate in a broadband range. The dependency of the spin shift with respect to the indicant angle, the thickness of air gap, and also the Fermi energy of graphene is discussed. By optimizing the thickness of air gap and the Fermi energy of graphene, the considerable spin shift in broadband range covering the terahertz, infrared and visible regions is realized around Brewster angle. The only difference is that the Brewster angle of infrared and visible range are both almost near 33.5°, while that in the terahertz range increases dramatically with incident frequency decreasing. Consequently, in this layered structure containing graphene, the tunable and enhanced SHE of light in broadband range is demonstrated, which may lead to some potential applications in developing new nanophotonic devices in broadband regions.

References

[1] Onada M, Murakami S and Nagaosa N 2004 *Phys. Rev. Lett.* **93** 083901
[2] Sinova J, Culcer D, Niu Q, Sinitsyn N A, Jungwirth T and Macdonald A H 2004 *Phys. Rev. Lett.* **92** 126603
[3] Bliokh K Y, Rodríguez-Fortuño F J, Nori F and Zayats A V 2015 *Nat. Photon.* **9** 796
[4] Bliokh K Y and Bliokh Y P 2006 *Phys. Rev. Lett.* **96** 073903
[5] Cardano F and Marrucci L 2015 *Nat. Photon.* **9** 776
[6] Bliokh K Y and Bliokh Y P 2007 *Phys. Rev. E* **75** 066609
[7] Bliokh K Y, Dressel J and Nori F 2014 *New J. Phys.* **16** 093037
[8] Hosten O and Kwiat P G 2008 *Science* **319** 787
[9] Menard J, Mattacchione A E, Betz M and Van Driel H M 2009 *Opt. Lett.* **34** 2312
[10] Aiello A and Woerdman J P 2008 *Opt. Lett.* **33** 1437
[11] Luo H L, Ling X H, Zhou X X, Shu W X, Wen S C and Fan D Y 2011 *Phys. Rev. A* **84** 033801
[12] Tang M, Zhou X X, Luo H L and Wen S C 2012 *Chin. Phys. B* **21** 124201
[13] Ling X H, Luo H L, Tang M and Wen S C 2012 *Chin. Phys. Lett.* **29** 074209
[14] Aiello A, Lindlein N, Marquardt C and Leuchs G 2009 *Phys. Rev. Lett.* **103** 100401
[15] Jiang X, Wang Q K, Guo J, Zhang J, Chen S Q, Dai X Y and Xiang Y J 2018 *J. Phys. D: Appl. Phys.* **51** 145104
[16] Li J, Tang T T, Luo L and Yao J Q 2018 *Carbon* **134** 293
[17] Zhang W S, Wu W J, Chen S Z, Zhang J, Ling X H, Shu W X, Luo H L and Wen S C 2018 *Photon. Res.* **6** 511
[18] Zhou X X, Ling X H, Xiao Z C, Low T, Alù A, Zhang B L and Sun H D 2019 *Phys. Rev. B* **100** 115429
[19] Jiang X, Tang J, Li Z F, Liao Y L, Jiang L Y, Dai X Y and Xiang Y J 2019 *J. Phys. D: Appl. Phys.* **52** 045401
[20] Tang M, Zhou X X, Xiao Z C, Luo H L and Wen S C 2013 *Chin. Phys. B* **22** 034101
[21] Qiu X, Zhang Z, Xie L, Qiu J, Gao F and Du J 2015 *Opt. Lett.* **40** 1018
[22] Zhu W G and She W L 2015 *Opt. Lett.* **40** 2961
[23] Luo L and Tang T T 2017 *Superlattice Microst.* **109** 259
[24] Tan X J and Zhu X S 2016 *Opt. Lett.* **41** 2478
[25] Qin Z R, Yue C, Lang Y P and Liu Q G 2018 *Opt. Commun.* **426** 16
[26] Xiang Y J, Jiang X, You Q, Guo J and Dai X Y 2017 *Photon. Res.* **5** 467
[27] Novoselov K S, Geim A K, Morozov S V, Jiang D, Zhang Y, Dubonos S V, Grigorieva I V and Firsov A A 2004 *Science* **306** 666
[28] Hu H, Zhai F, Hu D B, Li Z J, Bai B, Yang X X and Dai Q 2015 *Nanoscale* **7** 19493
[29] Vakil A and Engheta N 2011 *Science* **332** 1291
[30] Bai X X, Tang L L, Lu W Q, Wei X Z, Liu S, Liu Y, Sun X D, Shi H F and Lu Y G 2017 *Opt. Lett.* **42** 4087
[31] Zhou X X, Ling X H, Luo H L and Wen S C 2012 *Appl. Phys. Lett.* **101** 251602
[32] Gao C and Guo B 2018 *Optik* **158** 850
[33] Cheng M, Fu P, Tang X T, Chen S Y, Chen X Y, LinY T and Feng S Y 2018 *J. Opt. Soc. Am. B* **35** 1829
[34] Wu Y D, Sheng L J, Xie L G, Li S X, Nie P, Chen Y, Zhou X X and Ling X H 2020 *Carbon* **166** 396
[35] Falkovsky L A and Pershoguba S S 2007 *Phys. Rev. B* **76** 153410
[36] Digital Library of Mathematical Functions, http://dlmf.nist.gov, National Institute of Standard and Technology 2010
[37] Zhan T R, Shi X, Dai Y Y, Liu X H and Zi J 2013 *J. Phys.: Conden. Matter* **25** 215301
[38] Jian A Q and Zhang X M 2013 *IEEE J. Sel. Top. Quantum.* **19** 9000310